Journal of Ceramic Processing Research. Vol. 7, No. 3, pp. 230~234 (2006)

J O U R N A L O F
Ceramic Processing Research

Characterization and superconducting properties of (YSN)BCO composites made a top-seeded melt growth process

So-Jung Kim*
Department of Electrical and Electronic Engineering, Hanzhong University, Donghae, Gangwon 240-713, Korea

We have investigated the crystal growth and superconducting properties of c-axis oriented $(Y_{0.5}Sm_{0.25}Nd_{0.25})Ba_2Cu_3O_y$ [(YSN)-123] composite oxides by a top-seeded melt growth (TSMG) process in air. A melt-textured $NdBa_2Cu_3O_y$ (Nd-123) single crystal was used as a seed for achieving the c-axis(001) alignment of large grains perpendicular to the surface of a (YSN)-123 composite. A sample prepared by this method showed a well-textured microstructure, and $(Y_{0.5}Sm_{0.25}Nd_{0.25})_2BaCuO_5$ [(YSN)211] nonsuperconducting particles were uniformly dispersed in large (YSN)123 superconducting matrix grains. The melt-textured (YSN)-123 sample showed an onset of the superconducting transition (T_c) at 93 K. The magnetization hysteresis (M-H) values (300 emu/cm^3 at 4 T and 60 K) of the (YSN)-123 sample exhibited enhanced flux pinning, compared with a $(RE_{0.5}Y_{0.5})Ba_2Cu_3O_y$ [(REY)-123, RE: Sm, Nd] sample.

Key words: $(Y_{0.5}Sm_{0.25}Nd_{0.25})Ba_2Cu_3O_y$, $NdBa_2Cu_3O_y$, single crystal, top-seeded melt growth, $(Y_{0.5}Sm_{0.25}Nd_{0.25})_2BaCuO_5$, $(RE_{0.5}Y_{0.5})Ba_2Cu_3O_y$, magnetization.

Introduction

The top-seeded melt growth (TSMG) process is widely used to grow well-oriented large single grain $YBa_2Cu_3O_y$(Y-123) and $REBa_2Cu_3O_y$ (RE-123, RE: Nd, Sm, Gd, etc.) pellets which are necessary for bulk applications such as energy storage systems, superconducting magnetic bearings and non-contact transport systems [1-6]. The high temperature REBCO (RE-123) single grain bulk superconductors are attractive for various engineering applications. Unlike the YBCO(Y-123) system, which only forms a stoichiometric Y-123 compound, an important drawback of these matrials is, however, that the actual composition exhibit a $RE_{1+x}Ba_{1-x}Cu_3O_y$ type solid solution. The key to high performance of the melt-textured REBCO system is to suppress the amount of RE elements occupying Ba lattice sites. Large single grain REBCO bulk superconductors with superior superconducting properties have been prepared by an oxygen-controlled melt growth (OCMG) process [7-9], which is a process using a reduced oxygen partial pressure (PO_2) atmosphere. However, from the viewpoint of batch production with considerably low cost, it is desirable that large samples with a high performance be melt processed in an air atmosphere. Different methods [10-13] have been developed to suppress the RE/Ba substitution and hence to improve the superconducting performance of the REBCO bulk superconductors melt processed in an ambient atmosphere. Such a preferred growth could also be realized using a Ba-rich initial composition to facilitate the crystallization. In this present work, we fabricated single grain (YSN)-123 bulk superconductors with enhanced superconducting properties through the complete substitution of the RE and Y composite oxides by adding liquid phase (Liq., $BaCuO_2$). Melt-textured (YSN)-123 samples could be grown by top seeded melt growth process under an ambient atmosphere and their superconducting properties are discussed.

Experimental Procedures

Nd-123 Seed Crystal Preparation

The nominal composition was taken as $NdBa_2Cu_3O_y$ (Nd123)+$Nd_4Ba_2Cu_2O_y$(Nd422). The powders were sintered twice at 900 °C and 1100 °C for 24 h in air, with intermediate grindings, to obtain Nd123 and Nd422, respectively. These powders of Nd123 and Nd422 were mixed to have a nominal composition of Nd123+30 mol.%Nd422. For melt-texturing NdBCO, the precursor powders were pressed into pellets 10 mm in diameter and 5 mm in thickness, which were then subjected to a cold isostatic press (CIP) treatment with a pressure of 200 MPa. The pressed samples were melt textured in a box furnace in a nominal air atmosphere. The heat treatment profile used in the present experiment was as follows. The sample was heated to a temperature of 50 °C above the peritectic temperature (T_p: 1086 °C in air) in 1 h and held for 1 h, then rapidly

*Corresponding author:
Tel : +82-33-520-9322
Fax: +82-33-521-9407
E-mail: sjkim-jerome@hanmail.net

cooled to 10 °C above T_p in 5 minutes, and slowly cooled to 950 °C with a cooling rate of 1 Kh^{-1} followed by furnace cooling.

Characterization of (YSN)-123 Single Crystals

Precursor powder was prepared from the raw materials of Y_2O_3, Sm_2O_3, Nd_2O_3, $BaCO_3$ and CuO. The amounts of these powders were calculated to ensure (YSN)123+ 40 mol.% (YSN)211+20 mol.%Liq. ($BaCuO_2$). The powders were mixed thoroughly by ball milling in acetone for 24 h and calcined subsequently at 900 °C for 30 h twice in air with an intermediate grinding. The calcined powders were attrition milled for 6 h in acetone using zirconia balls with a rotation speed of 450 rpm. The attrition-milled (YSN)-123 powders were dried in air and then isostatically pressed into a pellet with a diameter of 10 mm and height of 5 mm in an ethyl-alcohol chamber. For TSMG processing, the a-b(010) plane of the Nd-123 seed crystal was placed on the top of the (YSN)-123 pellet. A (001) MgO single crystal was used as the substrate. It was known that a TSMG process allows the growth of c-axis oriented REBCO bulk superconductors. A cold seeding method, in which a seed crystal is placed in a precursor thermal cycle, has the advantage that the technique is simple and does not require a special device for delivering a seed at high temperature compared as is needed in a hot seeding method [4, 5]. The samples were heat-treated according to the heat schedule shown in Fig. 1. For oxidation, the samples were heated to 400 °C for 100 h in an oxygen gas flow. The phases of the calcined powder and the melt-textured (YSN)-123 samples formed were identified by means of XRD analysis. The microstructure was examined by a scanning electron microscopy (SEM) and transmission electron microscopy (TEM). Superconducting properties were measured by a SQUID magnetometer (Quantum Design, MPMS-7).

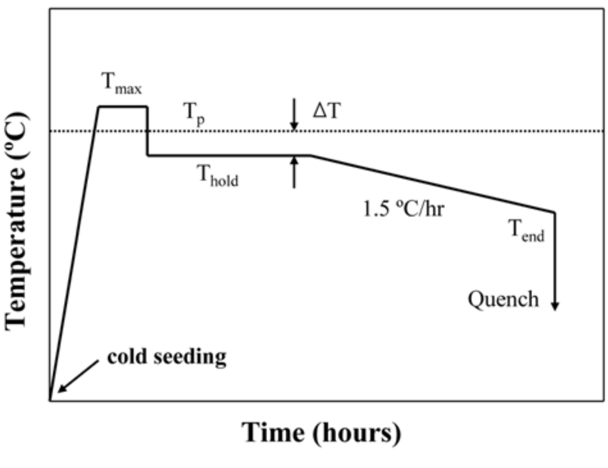

Fig. 1. Schematic illustration of the temperature profile for the (YSN)-123 composite oxides by the TSMG process. T_{max} and T_p are the maximum holding temperature and peritectic decomposition temperature estimated from DTA, respectively.

Results and Discussion

Fabrication of Single Grains in Air

For REBCO bulk superconductors prepared under an ambient atmosphere, the key issue is the effective suppression of RE-Ba substitution, which is vitally important for achieving superior superconducting properties. The peritectic temperature (T_p) of a (YSN)-123 sample in an air atmosphere is about 1065 °C. To keep this system melt-processed by the cold seeding method, T_p was used to determine the details (T_{max}, T_{hold} and T_{end}) of the thermal patterns for each. The details of the heating profile are summarized in Table 1. Figure 2 shows a typical top view of the (YSN)-123 sample grown using an a-b plane of a Nd-123 seed crystal. The (YSN)-123 crystal grew epitaxially from the Nd-123 seed crystal with a rectangular shape in the plane of pellet.

Microstructure Observations

The crystal growth modes were classified into several groups [4, 14, 15]. When T_{max} was optimum, a single grain was grown from the Nd-123 seed crystal without undesirable subsidiary nucreation as shown in Fig. 2. Figure 3 shows the single grain has a rectangular shape

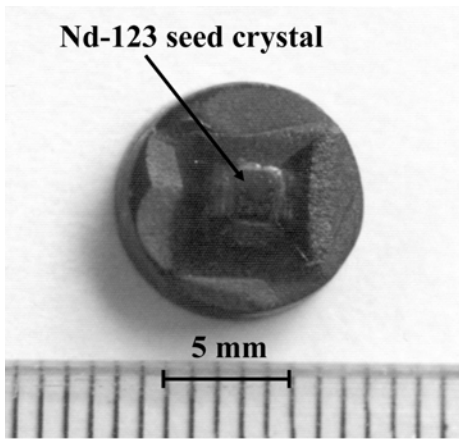

Fig. 2. A typical top view of the as grown (YSN)-123 sample using a Nd-123 seed crystal in air.

Table 1. Temperature details of thermal pattern for (YSN)-123 system

Maximum temperature, T_{max} (°C)	Peritectic temperature, T_p (°C)	Holding temperature, T_{hold} (°C)	Undercooling temperature, ΔT (T_p-T_{hold})	Superconducting transition temperature, T_c (K)
1100	1065	1050	15	93

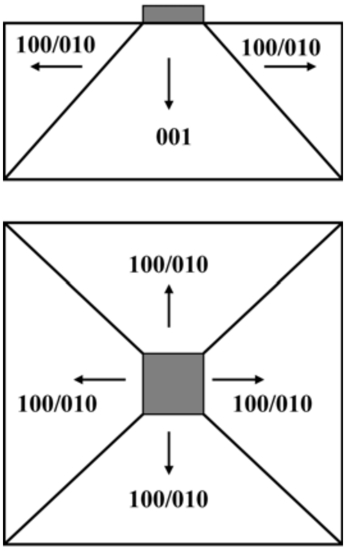

Fig. 3. Schematic illustrations for the TSMG processed single grain bulk with the c-axis parallel to the sample axis.

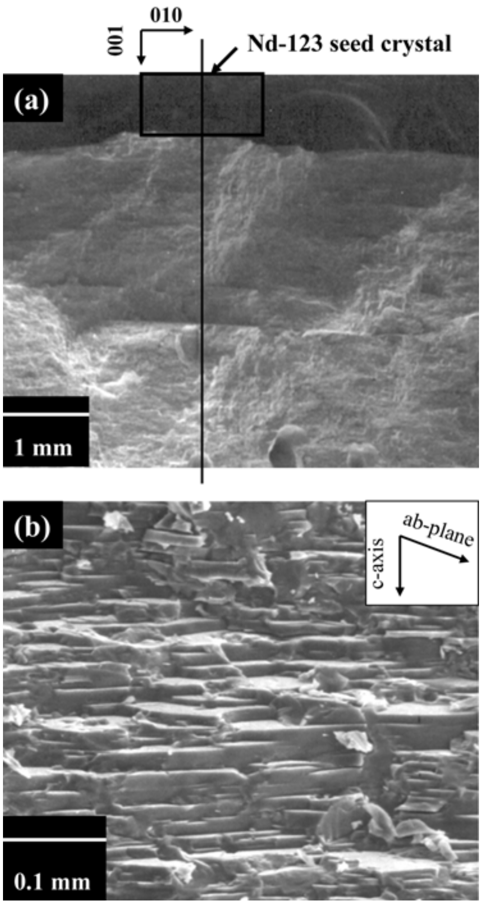

Fig. 4. SEM micrographs of the cross sectional views of the as-grown (YSN)-123 crystal: (a) lateral cross section and (b) is along the a-b, c direction.

due to the fact that the growth rates in the [100] and [110] directions are faster than in the [001] direction.

Figure 4 shows the cross sectional views of as-grown (YSN)-123 crystal viewed in Fig. 2. The (YSN)-123

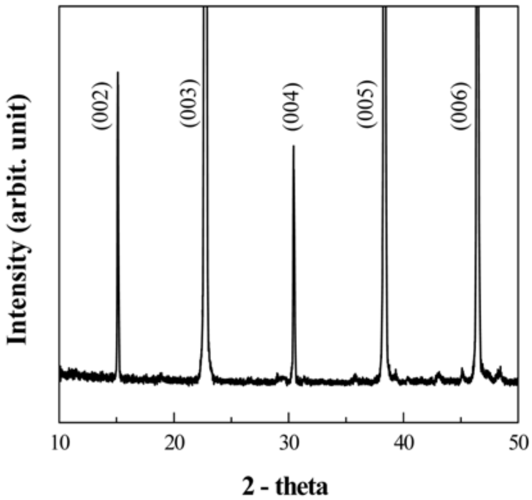

Fig. 5. The XRD pattern of the TSMG (YSN)-123 single crystal, showing the near perfect c-axis orientation.

crystal grew epitaxially from the Nd1.8 seed crystal with a rectangular shape in the plane of pellet. It is obvious that a (YSN)-123 composite single grain can be successfully fabricated with the Nd-123 seed crystal.

Figure 5 shows an XRD pattern of the cleavage surface of the melt-grown (YSN)-123 crystal. As shown in Fig. 5, there are only (00*l*) peaks, which means that the c-axis of the crystal is normal to the plane. Since no other phases are observed in this pattern, the grown crystal is a single phase of (YSN)-123.

A detailed microstructural analysis has been carried out by transmission electron microscopy (TEM) on the same samples. TEM was performed on a sample annealed at 400 °C for 100 h. After oxygen annealing, many defects are observed in the orthorhombic (YSN)123 matrix, especially around the trapped (YSN)211 inclusions. Figure 6 show [001] TEM bright field images of the melt-grown (YSN)-123 crystal. Figure 6(a) shows the microstructure around a (YSN) inclusion. It can be seen that fine (YSN)211 inclusions, spherical in shape, are observed in the (YSN)123 matrix. As can be seen in the Fig. 6(b), the existence of stacking faults and a high density of dislocations in addition to the twin structure are observed. Also, twin and twin boundaries having about a 50 nm spacing can be observed in Fig. 6(b).

The dislocations appear to be formed during cooling of the sample from the high temperature after the peritectic reaction or during the tetragonal-orthorhombic phase transformation. In the Y-Ba-Cu-O system, due to the difference in thermal expansion coefficient between Y211 and a Y123 phases, the dislocations might be formed during cooling of the sample because of the thermal stress evolved near the 123/211 interface [16]. Stacking faults were initiated at the (YSN)123/211 interface and then extended along the [100] and [010] directions of the (YSN)123 matrix. These stacking

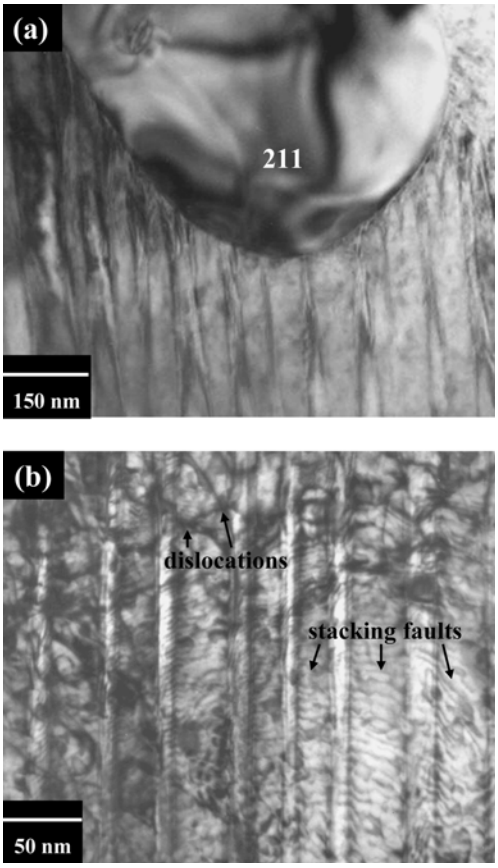

Fig. 6. TEM bright-field images of the TSMG (YSN)-123 crystal showing (a) (YSN)211 inclusion, (b) dislocation and stacking faults.

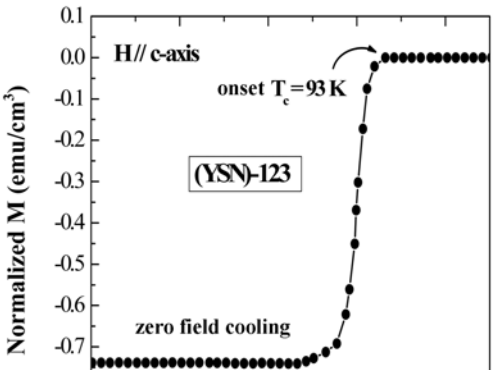

Fig. 7. Temperature dependence of dc magnetization of the TSMG (YSN)-123 crystal. The measurement was performed a with zero field cooled (ZFC) warming procedure and an applied field of 1 mT and for the H // c-axis direction.

faults, which have a structure with an extra Cu-O plane inserted in to the chain site of (YSN)123 matrix, may be the source of the flux pinning enhancement by (YSN)211 inclusions [2, 4], if the stacking faults are generated by introducing the inclusions.

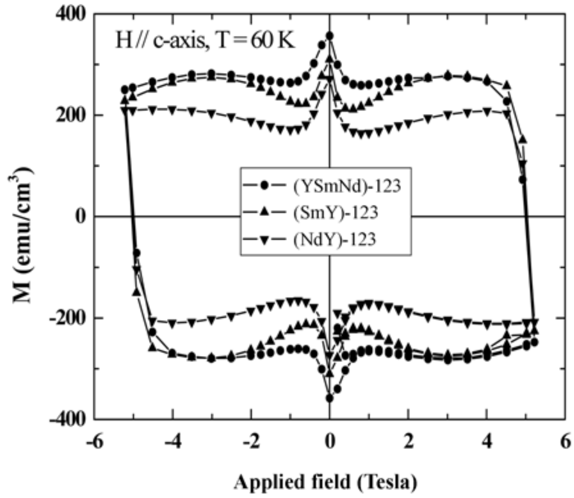

Fig. 8. Magnetization hysteresis (M-H) loops of the TSMG (YSN)-123 crystals.

Enhanced Superconducting Temperature and Magnetizations

A DC magnetization measurement was carried out using a quantum design SQUID magnetometer. Figure 7 shows the temperature dependence of magnetization of the (YSN)-123 composite single crystal. The field of 1 mT was applied parallel to the c-axis from 60 K to 110 K. In the melt-grown (YSN)-123 sample an onset $T_c \geq 93$ K and sharp transition were observed. This result is attributed to, in part, the finely dispersive (YSN)211 inclusions within the superconducting (YSN)123 matrix including microstructural defects such as microcracks, twins, dislocations and stacking faults which apparently act as effective pinning centers. For the analysis of flux pinning, magnetization hysteresis (M-H) loops of (YSN)-123 and (REY)-123 samples were measured as a function of the magnetic field (H//c-axis) up to 5 T.

A representative M-H loops at 60 K is shown in Fig. 8. The (YSN)-123 sample shows a larger magnetization hysteresis loop than that of melt-textured (REY)-123 sample. It is clear that the flux pinning mechanism by the complete substitution of RE/Y elements and the suppression of RE-Ba substitution via employing a Ba-rich initial composition in an ambient atmosphere is more effective in improving the superconducting properties (T_c, J_c) of the melt-textured (YSN)-123 composite.

Conclusions

In summary, we have succeeded in the syntheses of c-axis oriented (YSN)-123 composite superconductors by the TSMG process in an air atmosphere using Nd-123 as a seed crystal. A well-textured (YSN)-123 composite crystal grew epitaxially from the Nd-123 seed crystal with rectangular shape in the plane of pellet.

The melt-textured (YSN)-123 composite superconductors, showed an onset $T_c \cong 93$ K, and the magnetization hysteresis (M-H) values (300 emu/cm^3 at 4 T and 60 K) of the (YSN)-123 sample exhibited enhanced flux pinning.

References

1. S.J. Kim, K.W. Lee, and H.G. Kim, J. Crystal Growth 204 (1999) 78-82.
2. M. Muralidhar, M. Jirsa, N. Sakai, and M. Murakami, Supercond. Sci. Technol. 16 (2003) R1-16.
3. S. Nariki, N. Sakai, M. Murakami, and I. Hirabayashi, Supercond. Sci. Technol. 17 (2004) S30-35.
4. R. Cloots, T. Koutzarova, J.P. Mathieu, and M. Ausloos, Supercond. Sci. Technol. 18 (2005) R9-23.
5. Y. Shi, N. Hari Babu, and D. Cardwell, Supercond. Sci. Technol. 18 (2005) L13-L16.
6. S.J. Kim, J. Kor. Asso. Crystal Growth 15[4] (2005) 141-144.
7. M. Muralidhar, N. Sakai, M. Jirsa, and M. Murakami, Physica C 378 (2002) 646-650.
8. T. Yomada, H. Ikura, Y. Itoh, and U. Mizutani, Supercond. Sci. Technol. 16 (2003) 827-831.
9. A. Hu, N. Sakai, M. Murakami, and I. Hirabayashi, Supercond. Sci. Technol. 18 (2005) S52-S57.
10. A. Hu, N. Sakai, and M. Murakami, Physica C 386 (2003) 275-278.
11. J. Dai, Z. Zhau, and J. Xiong, Supercond. Sci. Technol. 16 (2003) 815-819.
12. J. Dai, Z. Zhau, and A. Hu, Physica C 406 (2004) 63-71.
13. M. Kambara, N. Hari Babu, D. A. Cardwell, and A. M. Campbell, Supercond. Sci. Technol. 16 (2003) 1286-1293.
14. Y. Shiohara and A. Endo, Mater. Sci. Eng. R19 (1997) 1-86.
15. P. Diko, K. Zmorayova, X. Granados, F. Sandiumenge, and X. Obradors, Physica C 384 (2003) 125-129.
16. C.J. Kim, H.W. Park, K.B. Kim, and G.W. Hong, Supercond. Sci. Technol. 8 (1995) 652-659.